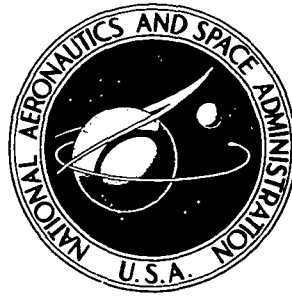


**NASA TECHNICAL  
MEMORANDUM**



**NASA TM X-2918**

**NASA TM X-2918**

**FLIGHT VELOCITY EFFECTS ON JET NOISE  
OF SEVERAL VARIATIONS OF A TWELVE-CHUTE  
SUPPRESSOR INSTALLED ON A PLUG NOZZLE**

*by Richard R. Burley and Albert L. Johns*

*Lewis Research Center  
Cleveland, Ohio 44135*

1. Report No. NASA TM X-2918		2. Government Accession No.		3. Recipient's Catalog No.	
4. Title and Subtitle <b>FLIGHT VELOCITY EFFECTS ON JET NOISE OF SEVERAL VARIATIONS OF A TWELVE-CHUTE SUPPRESSOR INSTALLED ON A PLUG NOZZLE</b>				5. Report Date January 1974	
				6. Performing Organization Code	
7. Author(s) Richard R. Burley and Albert L. Johns				8. Performing Organization Report No. E-7449	
9. Performing Organization Name and Address Lewis Research Center National Aeronautics and Space Administration Cleveland, Ohio 44135				10. Work Unit No. 501-24	
				11. Contract or Grant No.	
12. Sponsoring Agency Name and Address National Aeronautics and Space Administration Washington, D.C. 20546				13. Type of Report and Period Covered Technical Memorandum	
				14. Sponsoring Agency Code	
15. Supplementary Notes					
16. Abstract Because of the relatively high takeoff speeds of supersonic transport aircraft, it is important to know whether the flight velocity affects the noise level of suppressor nozzles. To investigate this, a modified F-106B aircraft was used to conduct a series of flyover and static tests on a 12-chute suppressor installed on an uncooled plug nozzle. Comparison of flyover and static spectra indicated that flight velocity adversely affected noise suppressions of the 12-chute configurations.					
17. Key Words (Suggested by Author(s)) Flight velocity effect; Jet noise suppressors; Nozzle thrust; Propulsion systems; Plug nozzle			18. Distribution Statement Unclassified - unlimited		
19. Security Classif. (of this report) Unclassified		20. Security Classif. (of this page) Unclassified		21. No. of Pages 37	22. Price* \$3.00

Cat. 28

**Page Intentionally Left Blank**

# FLIGHT VELOCITY EFFECTS ON JET NOISE OF SEVERAL VARIATIONS OF A TWELVE-CHUTE SUPPRESSOR INSTALLED ON A PLUG NOZZLE

by Richard R. Burley and Albert L. Johns

Lewis Research Center

## SUMMARY

Because of the relatively high takeoff speeds of supersonic transport aircraft, it is important to know whether the flight velocity affects the noise level of suppressor nozzles. To investigate this, a series of flyover and static tests were conducted on a 12-chute suppressor installed on an uncooled plug nozzle. The effects of a hard-wall shroud, an acoustically treated shroud, and an acoustically treated plug were also studied. The tests were conducted using an F-106B aircraft modified to carry two underwing nacelles each containing a calibrated J85-GE-13 turbojet engine. Data were taken over a range of J85 engine power settings that resulted in relative jet velocities from 375 to 610 meters per second (1230 to 2000 ft/sec) at static conditions and from 341 to 533 meters per second (1120 to 1750 ft/sec) for flyover conditions.

Comparison of the adjusted flyover and static spectra at the acoustic angle that resulted in peak flyover noise indicated that flight velocity adversely affected noise suppression of the 12-chute suppressor. This effect was also observed when the hard-wall shroud was installed on the 12-chute suppressor. The frequency spectrum for the 12-chute suppressor in flyover contained very little low-frequency noise but somewhat more high-frequency noise than that for the baseline nozzle. The peak sound pressure level occurred at a frequency of 2500 hertz. Installing the acoustic shroud and plug attenuated the noise by as much as 9 decibels (re  $2 \times 10^{-6}$  N/m<sup>2</sup>) at a frequency of 2500 hertz.

When the acoustic data from the flyover tests were scaled from J85 engine size (0.23 scale) to a full-scale four-engine aircraft and extrapolated to a sideline distance of 648 meters (2128 ft) from an altitude of 305 meters (1000 ft), the bare 12-chute suppressor reduced the peak noise level relative to the baseline nozzle by 5 effective perceived noise decibels (EPNdB). This reduction was achieved with a thrust penalty of about 5 percent, which makes this the most effective of the 12-chute suppressor configurations tested. The greatest amount of noise reduction, 10 EPNdB, occurred with the acoustic shroud installed on the 12-chute suppressor. However, it was achieved with a thrust penalty of 20 percent.

## INTRODUCTION

During takeoff of supersonic transport aircraft, the dominant noise source is the high-velocity jet issuing from the exhaust nozzle. Acoustic characteristics of both unsuppressed and suppressor-type exhaust nozzles generally have been determined at static conditions (cf. refs. 1 to 3). However, the takeoff speed of supersonic aircraft can be as high as Mach 0.35 when maximum sideline noise is reached. Thus, it is important to know whether the flight velocity affects the noise and thrust of exhaust nozzles.

To gain some insight into this question, a series of flyover and static tests are being conducted on both unsuppressed and suppressor exhaust nozzles. Some results are reported in references 4 and 5. In reference 6, a study of the effect of flight velocity on three basic types of unsuppressed nozzles shows that flight velocity favorably affects the noise suppression of an auxiliary inlet ejector nozzle. Results for a 32-spoke suppressor (ref. 7) show an adverse effect of flight velocity on the noise suppression of this configuration.

Another attractive type of suppressor is the multichute configuration. The present investigation was conducted to determine whether flight velocity affects the noise and thrust of a 12-chute suppressor installed on an uncooled plug nozzle. The suppressor was tested with no shroud, with a hard-wall shroud, and with an acoustically lined shroud. The effect of acoustically treating the plug surface also was studied.

The tests were conducted using an F-106B aircraft modified to carry podded engines mounted near the aft lower surface of the wing with the exhaust nozzle extending beyond the wing trailing edge. The primary jet exhaust was provided by calibrated turbojet engines (J85-GE-13). The flyovers were conducted at an altitude of 91 meters (300 ft) and a Mach number of 0.4. Acoustic measurements were taken from a ground station directly beneath the flightpath. For static tests, the acoustic measurements were taken at a radial distance of 30.48 meters (100 ft) from the nozzle. Data were taken over a range of J85 engine power settings from part throttle to military rpm. These settings gave a range of relative jet velocities from 375 to 610 meters per second (1230 to 2000 ft/sec) at static conditions and from 341 to 533 meters per second (1120 to 1750 ft/sec) for flyover conditions.

## APPARATUS AND PROCEDURE

### Test Facility

Flyover and static tests were conducted with an F-106B aircraft modified to carry two underwing nacelles. The aircraft in flight is shown in figure 1. A schematic view of the nacelle-engine installation is shown in figure 2. The 63.5-centimeter (25-in.)

diameter nacelles were located at approximately 32 percent semispan with the exhaust nozzles extending beyond the wing trailing edge. Since the nozzle would interfere with normal elevon movement, a section of the elevon immediately above each nacelle was cut out and rigidly fixed to the wing. Each nacelle contained a calibrated J85-GE-13 afterburning turbojet engine. The nacelles had normal shock inlets with blunted cowl lips for the flyover tests. Secondary air to cool the engine and afterburner was supplied from the inlet and was controlled at the periphery of the compressor face by a calibrated rotary valve. For the static tests, the blunted cowl lips were replaced with a bell-mouthed-inlet, as shown in figure 3.

Each nacelle was attached to the wing by two links normal to the nacelle axis. The axial force was measured by a load cell attached to the wing as shown in figure 2. An accelerometer in the nacelle allowed the load cell to be compensated for acceleration. The axial force transmitted to the compensated load cell can be divided into two parts: (1) nacelle drag forward of the research nozzle, referred to as the tare force; and (2) research nozzle gross thrust minus drag. Gross thrust minus drag is determined by adding the tare force to the compensated load cell reading. The tare force was zero for static tests (ref. 6). For flyover tests, the tare force is the sum of the ram drag plus the skin friction drag on the nacelle and strut (ref. 6).

### Baseline Nozzle

The baseline nozzle used for this study was an unsuppressed plug nozzle shown in figure 4. It consisted of a  $10^\circ$  half-angle conical plug body and a primary flap with a  $14^\circ$  trailing edge. A plug nozzle generally has a translating outer shroud, which is retracted for efficient operation at the low pressure ratios for takeoff conditions. The present configuration simulates the shroud in this position. Further details of this nozzle design are given in reference 8. Acoustic and thrust results for flyover conditions are presented in reference 6.

### Suppressor Configurations

The suppressor configurations are shown in figure 5. The 12-chute primary, installed on the plug nozzle just discussed, is shown in figure 5(a-1). The geometric throat of this primary was at about the same axial station as the exit plane for the primary flap of the plug nozzle. A plug nozzle was selected for the suppressor tests because it provides good aerodynamic performance, its mechanical systems are relatively simple, and the plug body provides a place to stow retractable noise suppressors.

A schematic of the 12-chute primary is shown in figure 5(a-2). External air flows down the smoothly converging surfaces of the 12 chutes and mixes with the primary jets issuing from the 12 rectangular-shaped exits. Since this suppressor design is relatively bulky, it was presumed to be nonretractable. The ratio of the area circumscribing the mixing nozzle to the primary effective area is 3. Some acoustic and thrust results are given in references 4 and 5. Thrust performance of a 21.59-centimeter (8.5-in.) diameter cold-flow isolated model at both takeoff and supersonic cruise conditions is given in reference 9.

The hard-wall shroud installed on the 12-chute primary is shown in figure 5(b-1) and a schematic is shown in figure 5(b-2). The shroud, which had an outer diameter of 63.5 centimeters (25 in.) to be consistent with the nacelle diameter, was 56.7 centimeters (22.3 in.) long to simulate a translating shroud in its supersonic cruise position.

The 12-chute primary tested with an acoustically treated shroud and an acoustically treated plug is shown in figure 5(c). The acoustic treatment consisted of a perforated plate adjacent to the hot jet, a bulk absorber, and a solid backing plate. Baffle disks were used for structural integrity. They also kept the bulk absorber from axial movement and served as resonator walls. The stainless-steel perforated plate was 0.079 centimeter (0.031 in.) thick and had 0.198-centimeter (0.078-in.) diameter holes and a 23 percent open area. The bulk absorber was 0.028-centimeter (0.011-in.) diameter stainless-steel wire mesh that filled each cavity to a density of  $322 \text{ kg/m}^3$  ( $20 \text{ lb/ft}^3$ ).

The acoustic shroud, which was the same length as the hard-wall shroud, had a maximum cavity depth of 2.97 centimeters (1.17 in.). This resulted in a shroud exit diameter of 57.18 centimeters (22.51 in.). The outer surface of the shroud had a boattail angle of  $15^\circ$  and a boattail juncture radius of 0.24 nacelle diameter. Because the absorber is the bulk type and because it is exposed to high gas flow velocities and sound pressure levels, the liner probably will act as a broadband absorber (ref. 10).

The acoustic plug was truncated to 80 percent of its full length. This amount of truncation should not significantly affect thrust performance (ref. 8). The acoustic treatment was applied to the exposed surface of the plug, resulting in a lining length of 75 centimeters (29.5 in.). The cavity depth varied from a maximum of 15 centimeters (5.8 in.) to a minimum of 1.55 centimeters (0.6 in.). This liner will probably also act as a broadband absorber.

#### Instrumentation

An onboard digital data system was used to record pressures, temperatures, and load cell output on magnetic tape. It had the capability of recording 578 parameters in 11.5 seconds (ref. 11). A flight-calibrated test boom located on the aircraft nose was used to determine free-stream static and total pressure, aircraft angle of attack, and

yaw angle. Aircraft altitude was determined by an onboard radio altimeter and a barometric altimeter, along with ground-based radar. Aircraft velocity was obtained from a calibrated Mach meter. The output of the Mach meter was sampled and recorded six times in about 11.5 seconds by the onboard digital data system.

Engine airflow was determined by using the calibration results from reference 12, along with measurements of engine speed and total pressure and temperature at the compressor face. Fuel flows were obtained from calibrated flowmeters. Total temperature  $T_8$ , total pressure  $P_8$ , and effective area  $A_8$  at the primary nozzle exit were obtained by using the values of engine airflow and fuel flow, the measured values of total pressure and temperature at the turbine discharge, and afterburner temperature rise and pressure drop calibration results from reference 12. Calibration of the secondary-flow-valve pressure drop and position were used to determine secondary airflow.

Total pressure and temperature of the secondary air were obtained from the probes shown in figure 6. Nozzle instrumentation is shown in figure 7. The 12-chute primary contained a row of six static pressure orifices at  $0^\circ$ ,  $90^\circ$ ,  $180^\circ$ , and  $270^\circ$  (fig. 7(a)). One static pressure orifice was located internally 1.27 centimeters (0.50 in.) from the shroud exit at  $0^\circ$ ,  $90^\circ$ ,  $180^\circ$ , and  $270^\circ$  (fig. 7(b)).

The noise-measuring instrumentation used in these tests is shown in the block diagram of figure 8. The microphone was a 2.54-centimeter (1-in.) diameter ceramic type. Frequency response of the microphone was flat to within  $\pm 2$  decibels for grazing incidence over the frequency range used. The output of the microphone was recorded on a two-channel direct-record tape recorder. The entire system was calibrated for sound level in the field before and after each test with a conventional tone calibrator. The tape recorder was calibrated for linearity with a "pink" noise (constant energy per octave) generator.

The flyover signal recorded on magnetic tape was played back through 1/3-octave-band filters and then reduced to digital form (fig. 8(b)). The averaging time used for data reduction was 0.1 second. The digital results were recorded on a tape. The time history of each flyover (in terms of PNL) and three associated frequency spectra (at peak perceived noise level and at 10 PNdB down from the peak on either side) were automatically plotted.

The static signal recorded on magnetic tape was played back through 1/3-octave-band filters, and the spectra were automatically plotted (fig. 8(c)). The averaging time used during data reduction was 0.125 second. The plotted results were converted into digital form and recorded on tape.

Meteorological conditions in terms of dry-bulb and dewpoint temperatures, wind speed and direction, and barometric pressure were recorded periodically throughout the test. Wind speeds were less than 5.144 meters per second (10 knots) during the tests.

## Procedure

The microphone stations for the acoustic measurements at static conditions are shown in figure 9. The measurements were made at a radial distance of 30.48 meters (100 ft) from the nozzle exit in increments of  $10^\circ$  over a  $90^\circ$  sector. The portable microphone was positioned 1.22 meters (4 ft) above the concrete surface and was oriented to receive the acoustic pressure waves at normal incidence, as shown in figure 9(a). It was fitted with a wind screen that caused no loss of signal. During the measurements, the main J75 engine was at idle power. The J85 in the nacelle containing the research nozzle was operated over a range of power settings, and the J85 engine in the other nacelle was shut off.

Background noise levels for the static tests were determined with both J85 engines shut off, the J75 engine at idle power, and external cooling air on. It was necessary to supply air from an external source to cool the J85 engine when it was operating at military power setting. The cooling air was supplied from an air start cart which was located on the far side of the aircraft, as shown in figure 10. The supply line went from the start cart to the J85 engine, and the air was directed around the engine through a nozzle (fig. 3). The J75 engine had to be operating when static data were taken because it supplied the electrical power for the onboard digital data system.

The background noise spectra (i. e. , with the J75 engine at idle power and the external air on) at acoustic angles of  $30^\circ$ ,  $40^\circ$ , and  $50^\circ$  are presented in reference 6. These spectra were adjusted to a standard day but not to free-field conditions. For all these angles, the levels adjusted to free field gradually increased to about 87 decibels at 1000 hertz and remained fairly constant until, at a frequency of 2500 hertz, they started to decrease. They reached a level of about 77 decibels at a frequency of 10 000 hertz. The background levels are sufficiently low so they do not interfere with the noise of the supersonic nozzles.

Acoustic measurements of the flyover noise were made from a ground station directly under the flightpath. The position of the microphone is shown in figure 11(a). It was positioned 1.22 meters (4 ft) above the concrete surface. The microphone, which was fitted with a wind screen that caused no loss of signal, was oriented to receive the acoustic pressure waves at grazing incidence.

The geometry of the flyover is shown in figure 11(b). As the aircraft travels along its flightpath, the direct ray distance from the nozzle to the microphone  $R_p$  continuously changes. The angle between the direct ray and the jet exit centerline, referred to as the acoustic angle  $\theta$ , also changes. The values of  $R_p$  and  $\theta$  are related to the sound data taken at a particular instant of time by having a ground observer manually record a signal on the tape (fig. 8(a)) as the aircraft passes directly over the microphone.

The flyovers were conducted at a Mach number of 0.4 and an altitude of 91 meters (300 ft). (See ref. 6 for the discussion concerning the selection of this altitude.) The

main engine of the aircraft was at idle power while the data were being recorded. The J85 engine in the nacelle that contained the research nozzle was operated at military and part power settings. The J85 engine in the opposite nacelle was shut off and allowed to windmill.

Background noise level during flyover was determined with the main engine at idle power and both J85 engines shut off and allowed to windmill. The results are presented in reference 6 and are adjusted to a standard day but not to free-field conditions. At an acoustic angle of about  $50^{\circ}$  (which, as is shown in the section Acoustic Characteristics, is about where the suppressor nozzles reach their peak noise level), the background noise level adjusted to free-field conditions is about 94 PNdB. The associated frequency spectrum has a fairly flat shape over most of the frequency range. The level, adjusted to free field, is about 68 decibels at frequencies below about 2000 hertz and decreases to about 57 decibels at a frequency of 10 000 hertz. These levels are sufficiently low so they do not interfere with noise from the suppressor nozzles.

## RESULTS AND DISCUSSION

### Acoustic Characteristics

To investigate whether flight velocity affects the noise of the 12-chute suppressor configurations, the measured flyover and static spectra were adjusted to comparable conditions: 30.48 meters (100 ft) from the nozzle in the free field on a standard day. The Doppler shift of frequency was accounted for in the flyover data spectra, and caused a maximum shift of one 1/3-octave band. Details of the adjustments are given in reference 6. The adjusted flyover and static spectra then were compared at a constant relative jet velocity of 533 meters per second (1750 ft/sec) and for the acoustic angle that resulted in peak flyover noise. Significant differences between the adjusted spectra would be attributed to flight velocity effects.

In making the comparison, the greatest emphasis should be placed on the data at frequencies between 160 and 5000 hertz. At frequencies below 160 hertz, the short integration time, the narrowness of the frequency bands, and the rapidly changing conditions of the flyover combine to give results that are not reliable. At frequencies above 5000 hertz, the acoustic signal received at the ground station quite possibly is below the noise floor of the recording equipment (ref. 13). Values of the atmospheric absorption coefficient are very large at these high frequencies and multiply the noise floor to unrealistically high noise levels in correcting the data to 30.48 meters (100 ft).

The flyover and static spectra for the 12-chute suppressor nozzle are compared in figure 12. The flyover spectrum is markedly higher than the static spectrum for frequencies greater than 630 hertz. This results in an overall sound pressure level

(OASPL) and a perceived noise level (PNL) about 3 decibels higher for the flyover than for the static spectrum. It suggests that flight velocity adversely affects the noise suppression of this nozzle.

The flyover and static spectra for the 12-chute suppressor nozzle with a hard-wall shroud are compared in figure 13. The flyover spectrum is somewhat below the static spectrum from 160 to 630 hertz but considerably above it at the higher frequencies. This results in an OASPL about 5 decibels higher and a PNL about 4 PNdB higher for the flyover than for the static spectrum. It suggests that flight velocity also had an adverse effect on the 12-chute suppressor with a hard-wall shroud.

Another indication of flight velocity effect is directivity and peak noise level. In figure 14 the variation in perceived noise level with acoustic angle during a typical flyover at an altitude of 91 meters is compared with that predicted from static data extrapolated to a 91-meter sideline. Figure 14(a) shows the results for the 12-chute suppressor nozzle. The flyover noise level reached a peak value of about 116.5 PNdB at an angle of about  $40^{\circ}$ . The static results predicted a somewhat lower peak value (115 PNdB) occurring about  $10^{\circ}$  further away from the jet axis. Figure 14(b) shows the results for the 12-chute suppressor with a hard-wall shroud. The flyover noise level reached a peak value of about 115.5 PNdB at an angle of about  $50^{\circ}$ . Again the static results predicted a lower peak value (114 PNdB) occurring about  $15^{\circ}$  farther away from the jet axis. Thus, for both configurations, the peak noise level predicted from static data was lower and occurred further away from the jet axis than that obtained during flyover.

The results of the flyover tests for all the suppressor configurations are presented in figure 15 in terms of the variation in perceived noise level with acoustic angle. For comparison, the results for the unsuppressed plug nozzle, used as the baseline nozzle, are also shown. The results are presented at a relative jet velocity of 533 meters per second. The background noise level, discussed in the section APPARATUS AND PROCEDURE, is also shown.

The baseline nozzle had a peak noise level of 117 PNdB occurring at an acoustic angle of  $40^{\circ}$ . The peak noise level of the 12-chute primary was about the same as that of the baseline nozzle but occurred about  $10^{\circ}$  farther away from the jet axis. Acoustically treating the plug surface did not have a significant effect on either the peak noise level or the angle at which it occurred. However, the noise level did seem to increase relative to the baseline nozzle at high acoustic angles for reasons that are not yet known. Using the hard-wall shroud with the 12-chute suppressor reduced the peak noise level about 1 PNdB but did not affect the angle at which it occurred. Acoustically treating the shroud surface resulted in a substantial reduction, about 6 PNdB, in the peak noise level but only a minor increase, about  $5^{\circ}$ , in the associated acoustic angle compared with the bare 12-chute suppressor. Theoretically (ref. 10), a greater amount of attenuation could be achieved by having the treated surface of the shroud parallel to the treated surface of the

plug (that is, rotate the shroud  $10^{\circ}$  toward the plug). The effect this would have on thrust performance is discussed in the section Thrust Characteristics.

The results just discussed were for a constant relative jet velocity. The effect that decreasing the relative jet velocity has on the peak flyover noise level is shown in figure 16. By comparing the results for a particular suppressor configuration to that for the baseline nozzle, the effectiveness of that particular suppressor as a function of relative jet velocity can be determined. Reducing the relative jet velocity adversely affected the suppression of the 12-chute primary. This was also the case when the hard-wall shroud was used. Both these configurations appeared to be noisier than the baseline nozzle at relative jet velocities less than about 480 meters per second (1580 ft/sec). Suppression of the 12-chute primary with the acoustic shroud and plug also was adversely affected by reducing the relative jet velocity. Thus, all the suppressor configurations lost effectiveness as relative jet velocity decreased.

The reason for this is associated with the noise floor that is being reached. This noise floor is different than the one previously mentioned, which was the result of the aircraft flying over with the main engine at idle power and both J85 engines shut off and allowed to windmill. This new noise floor is probably the result of internally generated noise from the J85 engine. This noise is considered to be associated with the highly turbulent flow inside the engine tailpipe and exhaust nozzle (ref. 14). It is not yet clear whether this noise is produced at flow obstructions (e.g., turbine cone, flameholder, etc.) or as the result of the increased flow turbulence at the nozzle exit modifying the external mixing noise (ref. 15). But since this noise is proportional to the sixth power of jet velocity rather than the eighth power, it will dominate at low jet velocities.

Conventional noise suppressors appear to be ineffective in suppressing internally generated noise. Furthermore, the increased surface area of the suppressor becomes a liability because it results in an increase in the scrubbing noise relative to the baseline nozzle with its smaller surface area.

The 12-chute primary belongs to a large class of suppressors called "mixing nozzles" which subdivide the jet exhaust into many elemental jets having the same total effective exit area as the baseline nozzle. Jet noise radiated from mixing nozzles has a composite spectrum. The high-frequency portion is considered to be the noise generated close to the nozzle exit plane by the mixing of the elemental jets with the ambient air. The low-frequency portion is considered to be the noise generated after the elemental jets have merged into a large single jet farther downstream of the nozzle exit.

The flyover spectra for the 12-chute primary and its associated configurations are shown in figure 17 along with the spectrum for the baseline nozzle. The results are presented for a relative jet velocity of 510 meters per second and at the acoustic angle that gave peak flyover noise for the baseline nozzle. The spectrum for the 12-chute primary contains only a small amount of low-frequency noise compared to that for the baseline nozzle, suggesting that a considerable amount of external air was entrained into the large

single jet thereby reducing its velocity. In some of the low-frequency bands (e.g., 200 and 250 Hz), as much as 16 to 18 decibels reduction in sound pressure level was obtained. The 12-chute primary spectrum contains somewhat less high-frequency noise than that of the baseline nozzle, suggesting that a considerable amount of mixing of the elemental jets with the surrounding air has occurred. The high-frequency noise peaked at a frequency of about 2500 hertz. Acoustically treating the plug surface had little effect on the spectrum. This was also the case when the hard-wall shroud was used. Acoustically treating the shroud surface, however, resulted in lowering the spectrum level over a wide range of frequencies. At a frequency of 2500 hertz, the reduction amounted to 9 decibels. The acoustic shroud, as expected, acted as a broadband absorber because the absorption material was of the bulk type and because of the high sound pressure levels and gas flow velocities to which the liner was exposed.

### Thrust Characteristics

In addition to acoustic characteristics, thrust characteristics also are important. Thrust performance for all the suppressor configurations is presented in figure 18 in terms of nozzle gross thrust coefficient as a function of nozzle pressure ratio. Values of relative jet velocity are also indicated on the abscissas. To determine the thrust penalty, results for the baseline nozzle also are shown.

Thrust performance at static conditions is shown in figure 18(a). The baseline nozzle has a gross thrust coefficient of 0.99 at a nozzle pressure ratio of 2.1. Installing the 12-chute primary lowered the thrust coefficient to 0.927, a 6.4 percent reduction from the baseline nozzle at a pressure ratio of 2.1. A contributing factor is the increased wetted surface area (excluding base area) of the 12-chute primary over that of the baseline nozzle, which results in decreased internal thrust and increased external skin friction drag. Installing the hard-wall shroud lowered the thrust coefficient to 0.82, a reduction of 10.8 percent from the bare 12-chute primary at a nozzle pressure ratio of 2.1. This shroud, as mentioned in the section APPARATUS AND PROCEDURE, had an outer diameter consistent with the nacelle diameter and a length chosen to give high performance at supersonic cruise conditions. As a result, the shroud exit area was considerably greater than that required to properly expand the primary flow at low values of nozzle pressure ratio. This greater exit area, combined with insufficient entrainment of external air to prevent the primary flow from being overexpanded, caused the base pressures to be lower than ambient. Installing the acoustic shroud and plug gave a thrust coefficient of 0.835, a reduction of 9.7 percent from the bare 12-chute primary at a pressure ratio of 2.1. The loss is smaller than with the hard-wall shroud. The increase in thrust coefficient (compared to using the hard-wall shroud) due to the reduction in

overexpansion of the flow more than offsets the decrease in thrust caused by the jets impinging on the converging surface of the acoustic shroud. For all the suppressor configurations, thrust loss increased as nozzle pressure ratio decreased.

Thrust performance at flyover conditions is shown in figure 18(b). The baseline nozzle had a gross thrust coefficient of 0.965 at a pressure ratio of 2.4. Installing the 12-chute primary lowered the thrust coefficient to 0.92, a reduction of 4.7 percent from the baseline nozzle at a pressure ratio of 2.4. Acoustically treating the plug surface caused only a small penalty in gross thrust coefficient, 1.6 percent, relative to the 12-chute primary at a pressure ratio of 2.4. Incorporating an acoustic shroud and plug lowered the thrust coefficient to 0.775, a 15.8 percent reduction from the bare 12-chute primary at a pressure ratio of 2.4. Since the acoustic plug caused only a 1.6 percent loss, most of the reduction in thrust coefficient, 14.2-percent, resulted from the acoustic shroud causing the primary flow to overexpand. Incorporating the hard-wall shroud caused the greatest loss in thrust coefficient, 18.5 percent relative to the bare 12-chute primary at a pressure ratio of 2.4. With the shroud installed (either hard wall or acoustically treated), the thrust loss relative to the bare 12-chute primary remained fairly constant as pressure ratio decreased. For the other two suppressor configurations (12-chute primary and 12-chute primary with acoustic plug), thrust loss relative to the baseline nozzle first increased and then decreased as pressure ratio decreased.

Another important question concerns the effect of flight velocity on the thrust coefficient of the suppressor configuration. This effect is shown in figure 19, which was obtained by comparing the static and flyover results from figure 18. Figure 19(a) shows the comparison for the 12-chute primary. Flight velocity had only a small adverse effect on the thrust coefficient of this configuration at high nozzle pressure ratios (a decrease of 1.5 percentage points at a nozzle pressure ratio of 2.3). This result suggests that the ventilation for this configuration was almost as good for flyover as for static conditions probably because the chutes had smoothly convergent external surfaces rather than blunt surfaces. The adverse effect became more pronounced as the pressure ratio decreased.

Installing a shroud on the 12-chute primary, as mentioned in connection with figure 18, caused a thrust loss at both static and flyover conditions because the primary flow was overexpanded. As shown in figures 19(b) and (c), the effect of flight velocity was to increase the overexpansion loss. With the acoustic shroud, the thrust coefficient was reduced about 6 percentage points at a pressure ratio of 2.3 (fig. 19(b)); with the hard-wall shroud, the reduction was about 8 percentage points at a pressure ratio of 2.3 (fig. 19(c)). The adverse effect increased somewhat as pressure ratio was decreased.

As just mentioned, the acoustically treated shroud caused a large thrust loss because the primary flow was overexpanded. The overexpansion could be reduced by shortening the shroud length. But this would reduce the lining length which, in turn, would decrease the attenuation. A method of decreasing overexpansion without decreasing attenuation would be to rotate the shroud toward the plug. For no overexpansion, the

separation distance between the treated surfaces of the shroud and plug would be such as to maintain a constant annular area. This, as mentioned in connection with figure 15, would result in increased attenuation. Although rotating the shroud would increase the boattail surface and thereby increase drag, the thrust loss due to overexpansion would decrease. So there is probably some configuration that minimizes the total thrust loss. This configuration would have a greater amount of attenuation than the existing configuration.

The 12-chute primary, as mentioned in the section APPARATUS AND PROCEDURE, is relatively bulky and was presumed to be nonretractable. Thrust performance over a range of subsonic Mach numbers is shown in figure 20 in terms of nozzle gross thrust coefficient. Results for the baseline nozzle are also presented. The thrust coefficient increased with increasing Mach number and peaked at Mach 0.95. At this Mach number, a terminal shock is located just upstream of the nozzle assembly (ref. 8). As Mach number was increased above Mach 0.95, a sharp drop in thrust coefficient occurred as the shock moved off the nozzle. The thrust coefficient for the 12-chute primary follows the same general shape. Thrust loss varied from 3.7 to 4.4 percent as Mach number varied from 0.6 to 0.95. At supersonic cruise, this type of suppressor caused a  $1\frac{1}{2}$  percent loss in gross thrust coefficient (ref. 9), which might be excessive for most applications.

### Suppressor Effectiveness

The suppressor configurations tested were 0.23-scale (J85 engine size) models for a supersonic transport engine. To determine suppressor effectiveness, acoustic data from the flyover tests were scaled to full size (four 267-kN (60 000-lbf) thrust engines). This scaling was done by using the Strouhal number relation (ref. 16) and assuming that both the 0.23-scale and full-scale engines were operating with identical primary gas conditions of pressure ratio, total temperature, and gas composition. It was further assumed that the 0.23-scale and the full-scale suppressors were exposed to identical flight velocities and were influenced in an identical manner by flight velocity.

After being adjusted to free-field conditions (ref. 6) and to standard-day conditions (simplified procedure outlined in ref. 17), the full-scale acoustic results were extrapolated to a sideline distance of 648 meters (2128 ft) from an altitude of approximately 305 meters (1000 ft). This extrapolation accounted for inverse-square radiation and atmospheric absorption. From this full-scale spectrum, which occurs at a particular instant of time, values of OASPL and PNL can be obtained. The entire procedure is then repeated for a number of time points. Finally, a time history, in terms of PNL, can be constructed and a value of EPNL can be obtained (procedure outlined in ref. 17).

Suppressor effectiveness for all the configurations is presented in figure 21 in terms of effective perceived noise level (EPNL) suppression (in EPNdB) as a function of percent thrust loss (relative to the baseline nozzle). The results are shown for a Mach number of about 0.4 and a nozzle pressure ratio of 2.4 (relative jet velocity, 533 m/sec (1750 ft/sec)). The bare 12-chute primary was the most effective of the 12-chute configurations tested, resulting in a suppression of 5 EPNdB for 5 percent loss in thrust. The largest amount of suppression, 10 EPNdB, was achieved using the acoustically treated shroud and plug. However, it was achieved with a thrust loss of 20 percent.

In the previous discussion, suppression was given in terms of a parameter called effective perceived noise level (EPNL), the units of which are EPNdB. This parameter accounts for suppression due to the distance between the noise source and the observer. It also accounts for the duration of the noise as the aircraft flies past the observer - a longer duration noise being more annoying and therefore less favorable than a noise of shorter duration. The amount that each of these factors contributes to the suppression of the 12-chute suppressor is shown in figure 22. Also shown is the effect that scaling has on suppression. A suppression of 0.5 PNdB was achieved with the 0.23-scale 12-chute suppressor when it was flown over the measuring station at an altitude of 91 meters (300 ft) and a Mach number of 0.4. Scaling to full size resulted in a suppression of 2.2 PNdB. Although scaling from 0.23 size to full scale increases the suppression by 1.7 PNdB, this might be in error (due to experimental measurement difficulties that will be discussed).

The effect of distance was determined by using the full-scale results extrapolated to the sideline distance of 648 meters from an altitude of 305 meters. A suppression of 3 PNdB was achieved, compared to a suppression of 2.2 PNdB when the full-scale suppressor was flown at an altitude of 91 meters directly over the measuring station. So the 12-chute suppressor benefits slightly by increasing the distance between the noise source and the observer. The reason is that the spectrum of the suppressor contains somewhat more high-frequency noise than does the spectrum of the baseline nozzle and the atmosphere selectively attenuates the high-frequency noise.

The last effect studied was that of time duration. Noise from the suppressor nozzle has a shorter time duration and therefore the annoyance from this factor is less, by 2 EPNdB, than noise from the baseline nozzle. The noise level of the suppressor nozzle rises and falls more rapidly with time than does the noise level of the baseline nozzle, whose noise seems to linger over a longer duration.

Earlier in this section, it was mentioned that the increase in suppression might not be a real effect. Instead, it might be the result of the full-scale spectrum being inaccurate at the higher frequencies where the noise floor is above the acoustic signal. Since the scaling factor is 0.23, the measured data at a frequency of 10 000 hertz scale to 2300 hertz. Full-scale noise levels at frequencies greater than 2300 hertz were obtained by extrapolation of the measured spectra.

Since the effect of scaling on suppression might be in error, this same uncertainty affects the absolute levels of suppression due to distance and duration. However, the relative differences probably are correct.

## SUMMARY OF RESULTS

A series of flyover and static tests were conducted on a 12-chute suppressor installed on an uncooled plug nozzle. The effects of a hard-wall shroud, an acoustically treated shroud, and an acoustically treated plug were also studied. The primary jet exhaust was provided by a calibrated turbojet engine. Data were taken over a range of power settings, which resulted in relative jet velocities between 341 and 533 meters per second (1120 to 1750 ft/sec) for flyover conditions. The results of the investigation at a relative jet velocity of about 533 meters per second can be summarized as follows:

1. Comparison of the adjusted spectra at the acoustic angle that results in peak flyover noise indicates that flight velocity adversely affected the noise suppression of the 12-chute nozzle. This was also the case when the hard-wall shroud was used.
2. The variation in perceived noise level with acoustic angle during a typical flyover compared with that extrapolated from static data indicates that the peak noise level predicted from static data was lower and occurred farther away from the jet axis than that obtained during the flyover. This effect was observed for the 12-chute suppressor with and without the hard-wall shroud.
3. The peak noise level of the 12-chute suppressor in flyover was about the same as that of the baseline nozzle but occurred about  $10^{\circ}$  farther from the jet axis than for the baseline nozzle. (The peak noise level of the baseline nozzle was 117 PNdB, occurring at an angle of  $40^{\circ}$ .) The acoustic shroud reduced the peak noise level 6 PNdB with only a minor (less than  $5^{\circ}$ ) increase in the associated acoustic angle. The effect of the hard-wall shroud was minor, as was the effect of only acoustically treating the plug.
4. The frequency spectrum for the 12-chute suppressor in flyover contained only a small amount of low-frequency noise but a large amount of high-frequency noise. In some of the low-frequency bands, as much as a 16-decibel reduction in sound pressure level was obtained relative to the spectrum for the baseline nozzle. The peak sound pressure level occurred at a frequency of 2500 hertz. The acoustically treated shroud attenuated the sound pressure level by as much as 9 decibels at a frequency of 2500 hertz.
5. When the acoustic data from the flyover were scaled from J85 engine size (0.23 scale) to full scale and extrapolated to a sideline distance of 648 meters (2128 ft) from an altitude of 305 meters (1000 ft), the 12-chute suppressor reduced the noise level by 5 EPNdB (relative to the baseline nozzle). This reduction was achieved with a thrust

penalty of about 5 percent, thus making it the most effective of the 12-chute suppressor configurations tested. The greatest amount of noise reduction, 10 EPNdB, was obtained with the acoustical shroud installed on the 12-chute suppressor. However, it was achieved with a thrust penalty of 20 percent.

Lewis Research Center,  
National Aeronautics and Space Administration,  
Cleveland, Ohio, September 18, 1973,  
501-24.

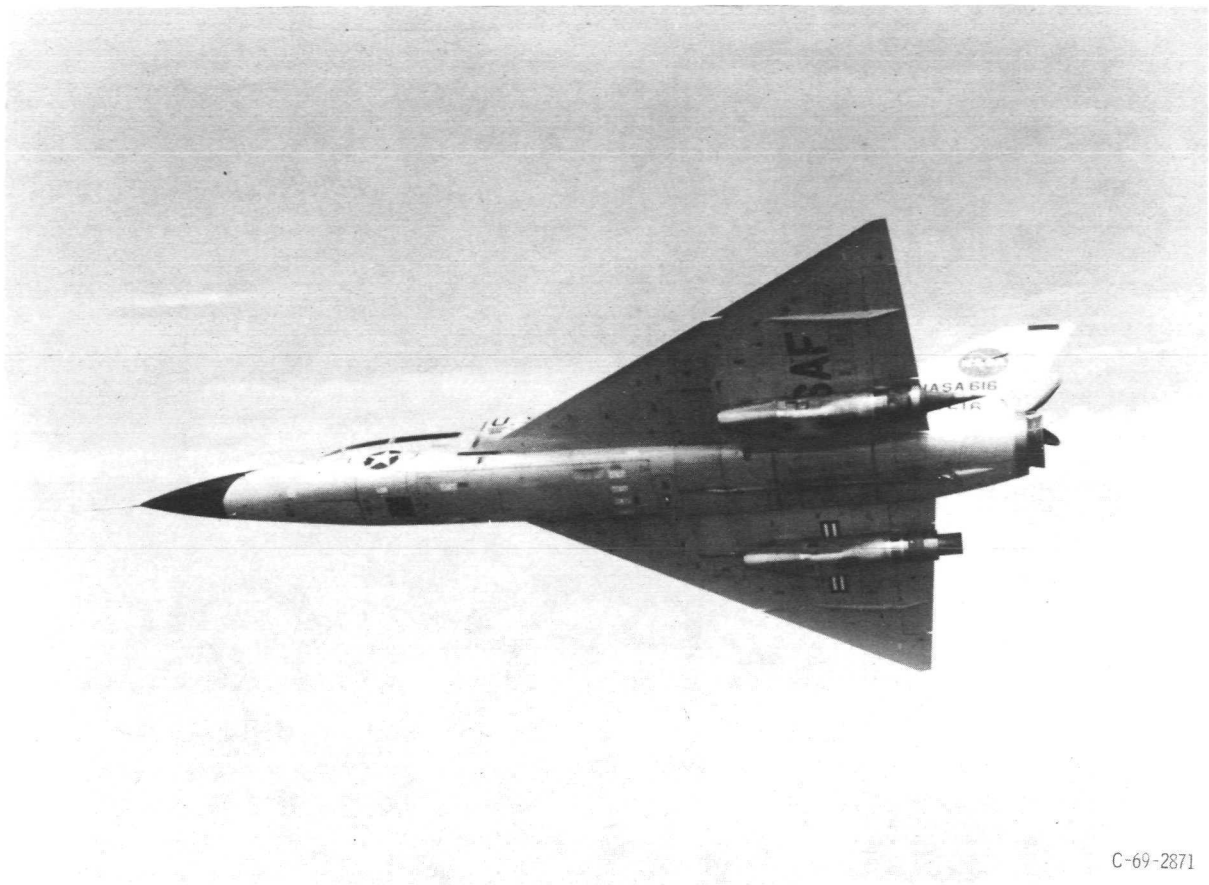
## APPENDIX - SYMBOLS

$A_8$	primary nozzle exit effective flow area (hot), $\text{cm}^2$ (in. <sup>2</sup> )
$D$	nozzle drag, kN (lbf)
db	decibel (re $2 \times 10^{-5} \text{ N/m}^2$ )
$d_n$	nacelle diameter, 63.5 cm (25 in.)
EPNL	effective perceived noise level, EPNdB
$F$	nozzle gross thrust, kN (lbf)
$F_{ip}$	ideal thrust of primary jet, kN (lbf)
$M_0$	flight Mach number
OASPL	overall sound pressure level, dB (re $2 \times 10^{-5} \text{ N/m}^2$ )
PNL	perceived noise level, PNdB
$P_8$	total pressure at primary nozzle exit, $\text{kN/m}^2$ (psia)
$P_8/p_0$	nozzle pressure ratio
$p_0$	ambient static pressure, $\text{kN/m}^2$ (psia)
$R_p$	direct ray distance, m (ft)
$r_\beta$	boattail junction radius, cm (in.)
$T_s$	total temperature of secondary air, K ( $^{\circ}\text{R}$ )
$T_8$	total temperature at primary nozzle exit, K ( $^{\circ}\text{R}$ )
$V_a$	aircraft velocity, m/sec (ft/sec)
$V_j$	ideal jet velocity, m/sec (ft/sec)
$V_r$	relative jet velocity, $V_j - V_a$ , m/sec (ft/sec)
$W_s$	secondary weight flow, kg/sec (lbm/sec)
$W_8$	weight flow at primary nozzle exit, kg/sec (lbm/sec)
$\theta$	acoustic angle, deg
$\omega \sqrt{\tau}$	corrected secondary weight flow ratio, $\frac{W_s}{W_8} \sqrt{\frac{T_s}{T_8}}$

## REFERENCES

1. Darchuk, George V. ; and Balombin, Joseph R. : Noise Evaluation of Four Exhaust Nozzles for Afterburning Turbojet Engines. NASA TM X-2014, 1970.
2. Huff, Ronald G. ; and Groesbeck, Donald E. : Splitting Supersonic Nozzle Flow Into Separate Jets By Overexpansion Into a Multilobed Divergent Nozzle. NASA TN D-6667, 1972.
3. Ciepluch, Carl C. ; North, Warren, J. ; Coles, Willard D. ; and Antl, Robert J. : Acoustic, Thrust, and Drag Characteristics of Several Full-Scale Noise Suppressors for Turbojet Engines. NACA TN 4261, 1958.
4. Brausch, J. F. : Flight Velocity Influence on Jet Noise of Conical Ejector, Annular Plug, and Segmented Suppressor Nozzles. General Electric Co. (NASA CR-120961), August 1972.
5. Burley, Richard R. ; and Karabinus, Raymond J. : Flyover and Static Tests to Investigate External Flow Effect on Jet Noise From Nonsuppressor and Suppressor Exhaust Nozzles. NASA TM X-68161, 1972.
6. Burley, Richard R. ; Karabinus, Raymond J. ; and Freedman, Robert J. : Flight Investigation of Acoustic and Thrust Characteristics of Several Exhaust Nozzles Installed on Underwing Nacelles on an F106 Aircraft. NASA TM X-2854, 1973.
7. Chamberlin, Roger: Flyover and Static Tests to Study Flight Velocity Effects on Jet Noise of Suppressed and Unsuppressed Plug Nozzle Configurations. NASA TM X-2856, 1973.
8. Samanich, Nick E. ; and Chamberlin, Roger: Flight Investigation of Installation Effects on a Plug Nozzle Installed on an Underwing Nacelle. NASA TM X-2295, 1971.
9. Bresnahan, Donald L. : Internal Performance of a  $10^{\circ}$  Conical Plug Nozzle with a Multispoke Primary and Translating External Shroud. NASA TM X-2573, 1972.
10. Mangiarotty, R. A. ; Marsh, Alan H. ; and Feder, Ernest: Duct-Lining Materials and Concepts. Progress of NASA Research Relating to Noise Alleviation of Large Subsonic Jet Aircraft. NASA SP-189, 1968, pp. 29-52.
11. Groth, Harold W. ; Samanich, Nick E. ; and Blumenthal, Philip Z. : Inflight Thrust Measuring System of Underwing Nacelles Installed on a Modified F-106 Aircraft. NASA TM X-2356, 1971.
12. Antl, Robert J. ; and Burley, Richard R. : Steady-State Airflow and Afterburning Performance Characteristics of Four J85-GE-13 Turbojet Engines. NASA TM X-1742, 1969.

13. Little, John W. ; Miller, Robert L. ; Oncley, Paul B. ; and Panko, Raymond E. :  
Studies of Atmospheric Attenuation of Noise. NASA Acoustically Treated Nacelle  
Program. NASA SP-220, 1969, pp. 125-135.
14. Grande, E. : Exhaust Noise Field Generated in the JT8D Core Engine-Noise Floor  
Presented by the Internal Noise Sources. Presented at the Acoustical Society of  
America 82nd Fall Meeting, Denver, Colo. , Oct. 19-22, 1971.
15. Gordon, Colin G. : A Study of Exhaust Noise as it Relates to the Turbofan Engine.  
Progress of NASA Research Relating to Noise Alleviation of Large Subsonic Jet  
Aircraft. NASA SP-189, 1968, pp. 319-334.
16. Anon. : Jet Noise Prediction. Aerospace Information Rep. 876, SAE, July 10, 1965.
17. Anon. : Federal Aviation Regulations, Vol. III, Part 36, Noise Standards: Aircraft  
Type Certification. Dept. of Transportation, Federal Aviation Administration.



C-69-2871

Figure 1. - Modified F-106B aircraft in flight.

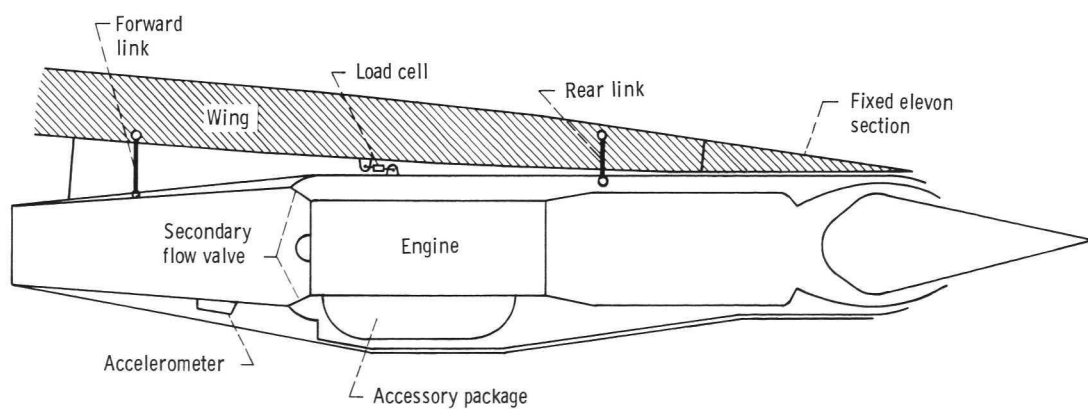
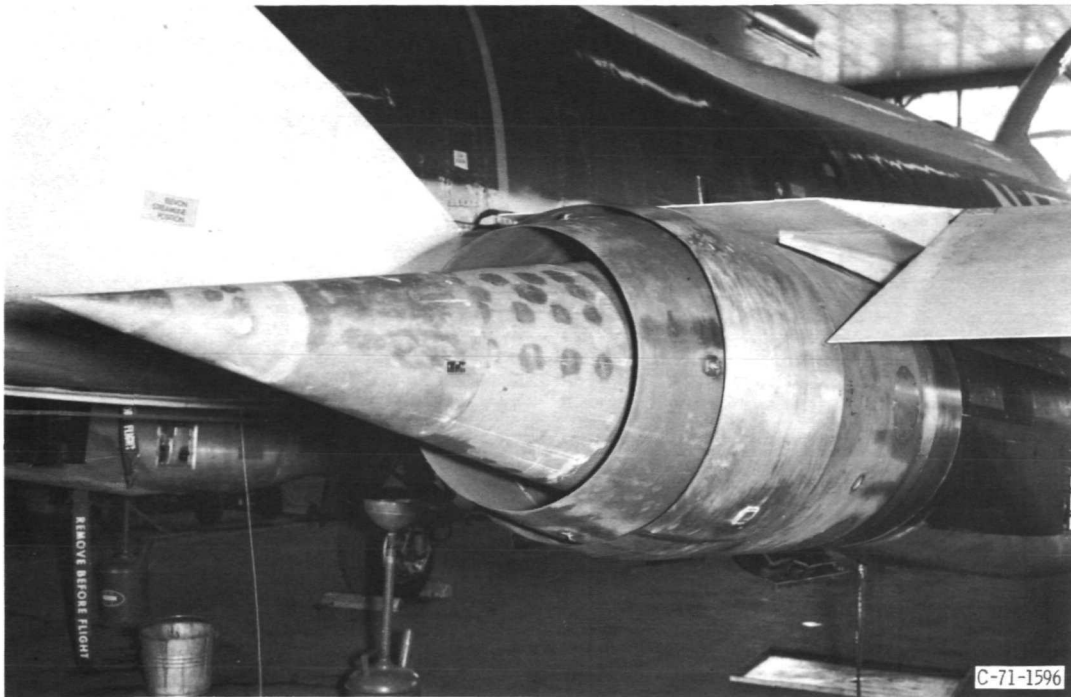


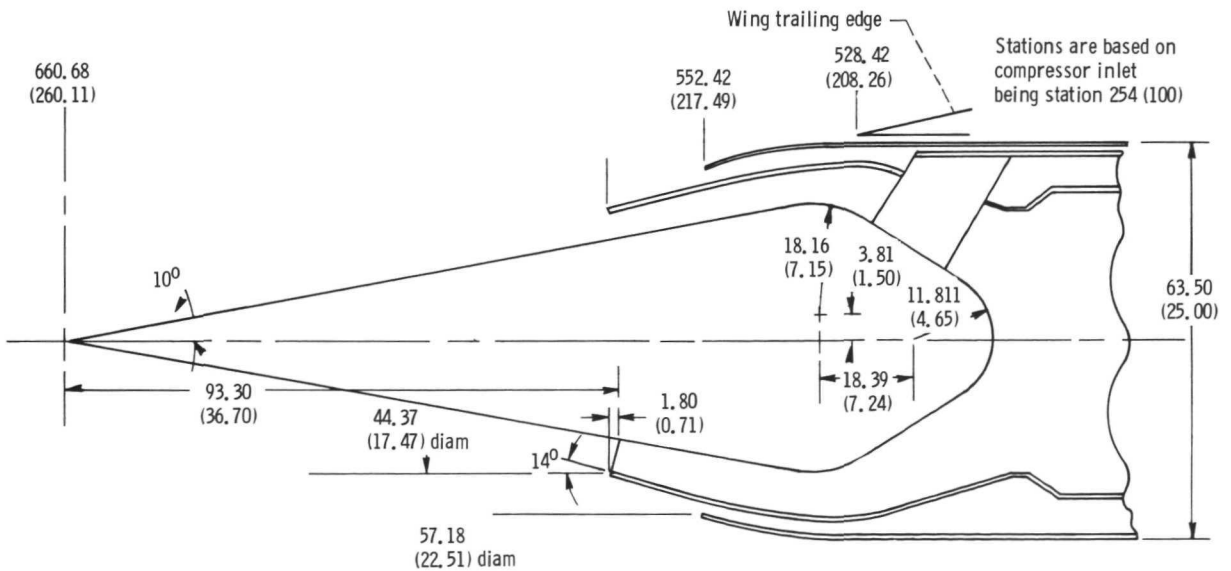
Figure 2. - Nacelle-engine installation.



Figure 3. - Nacelle modification for static tests.

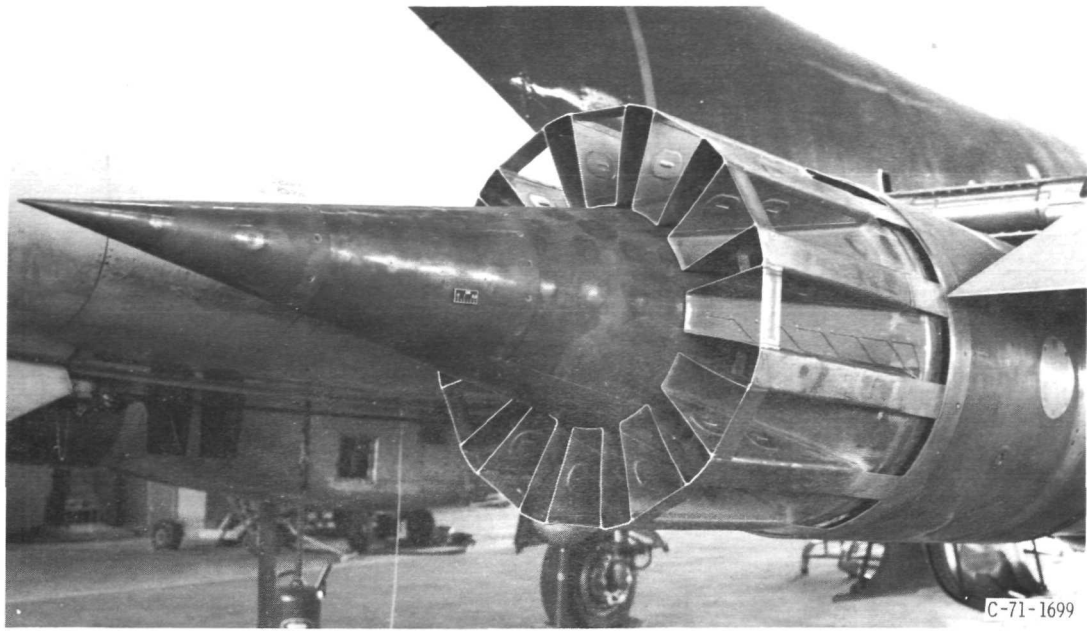


(a) Installed.

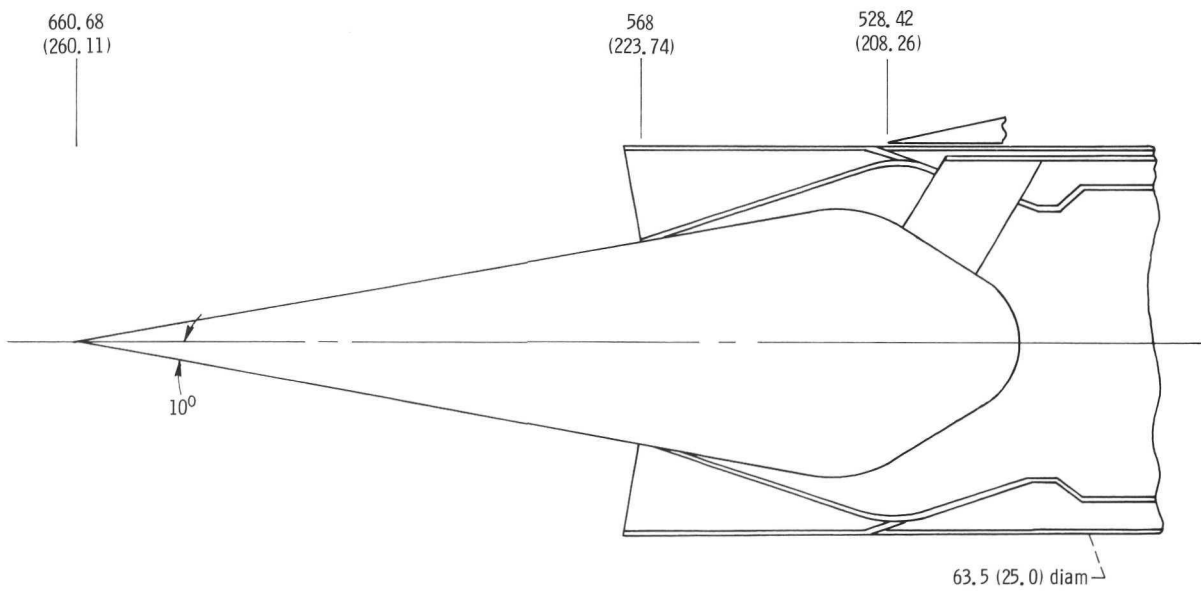


(b) Dimensional characteristics. (Dimensions are in cm (in.))

Figure 4. - Baseline nozzle.



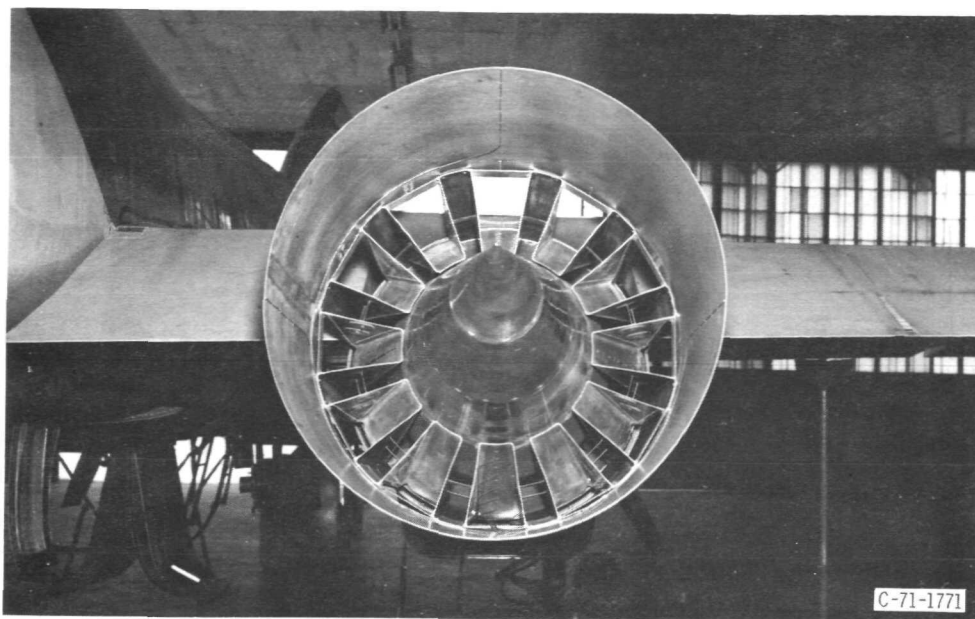
(a-1) Installed.



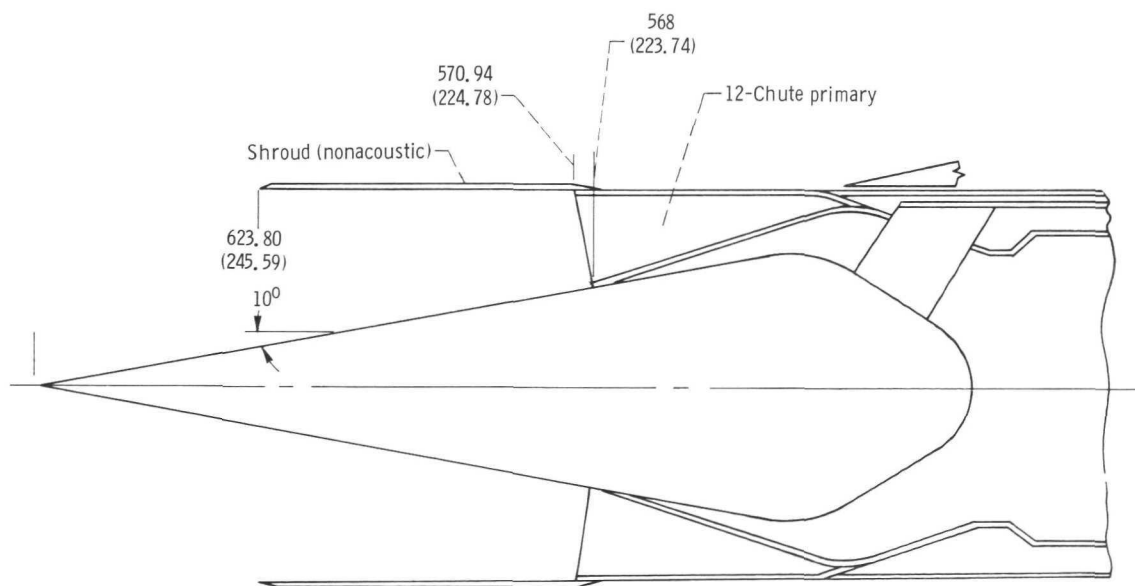
(a-2) Dimensional characteristics. (Dimensions are in cm (in.))

(a) Twelve-chute primary.

Figure 5. - Twelve-chute configurations.



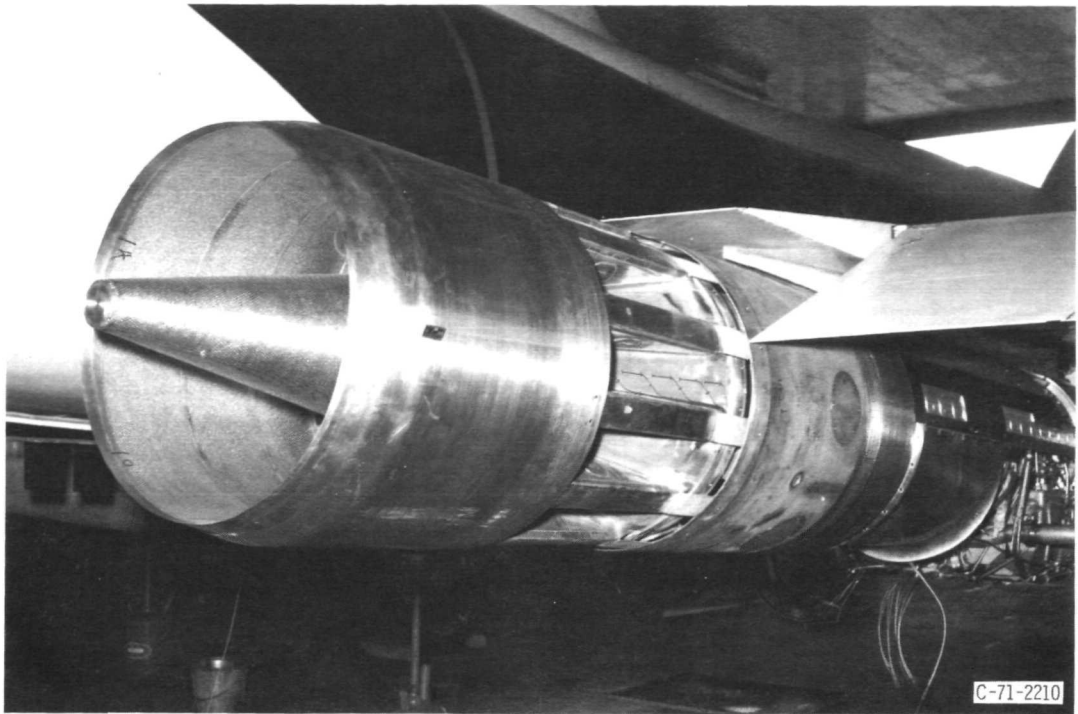
(b-1) Installed.



(b-2) Dimensional characteristics. (Dimensions are in cm (in. ), )

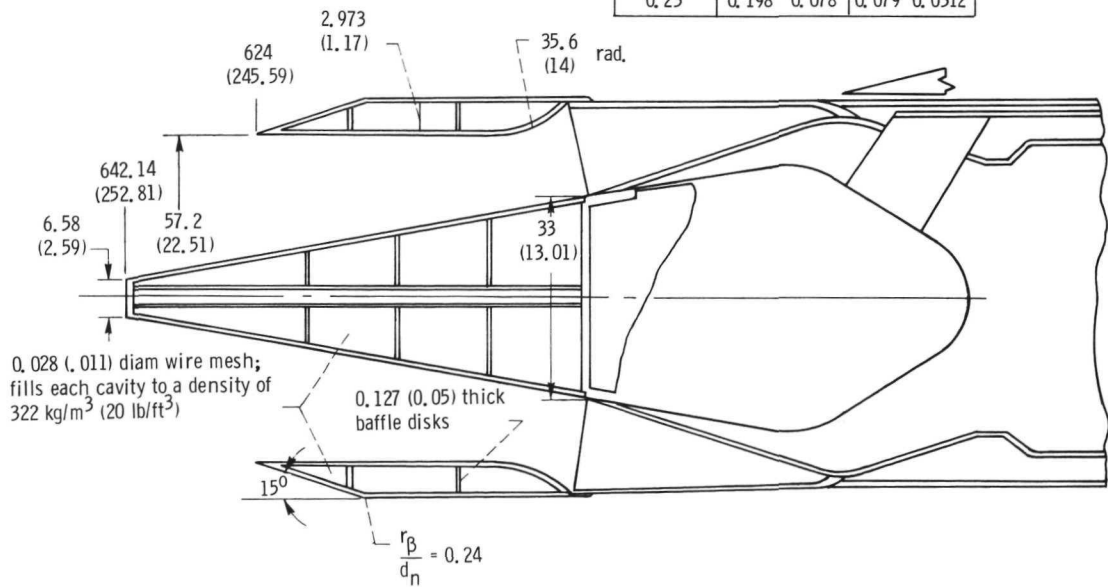
(b) Twelve-chute primary with hard-wall shroud.

Figure 5. - Continued.



(c-1) Installed.

Perforated plate				
Open-area ratio	Hole diameter		Thickness	
	cm	in.	cm	in.
0.23	0.198	0.078	0.079	0.0312



(c-2) Dimensional characteristics. (Dimensions are in cm (in.))

(c) Twelve-chute primary with acoustic plug and shroud.

Figure 5. - Concluded.

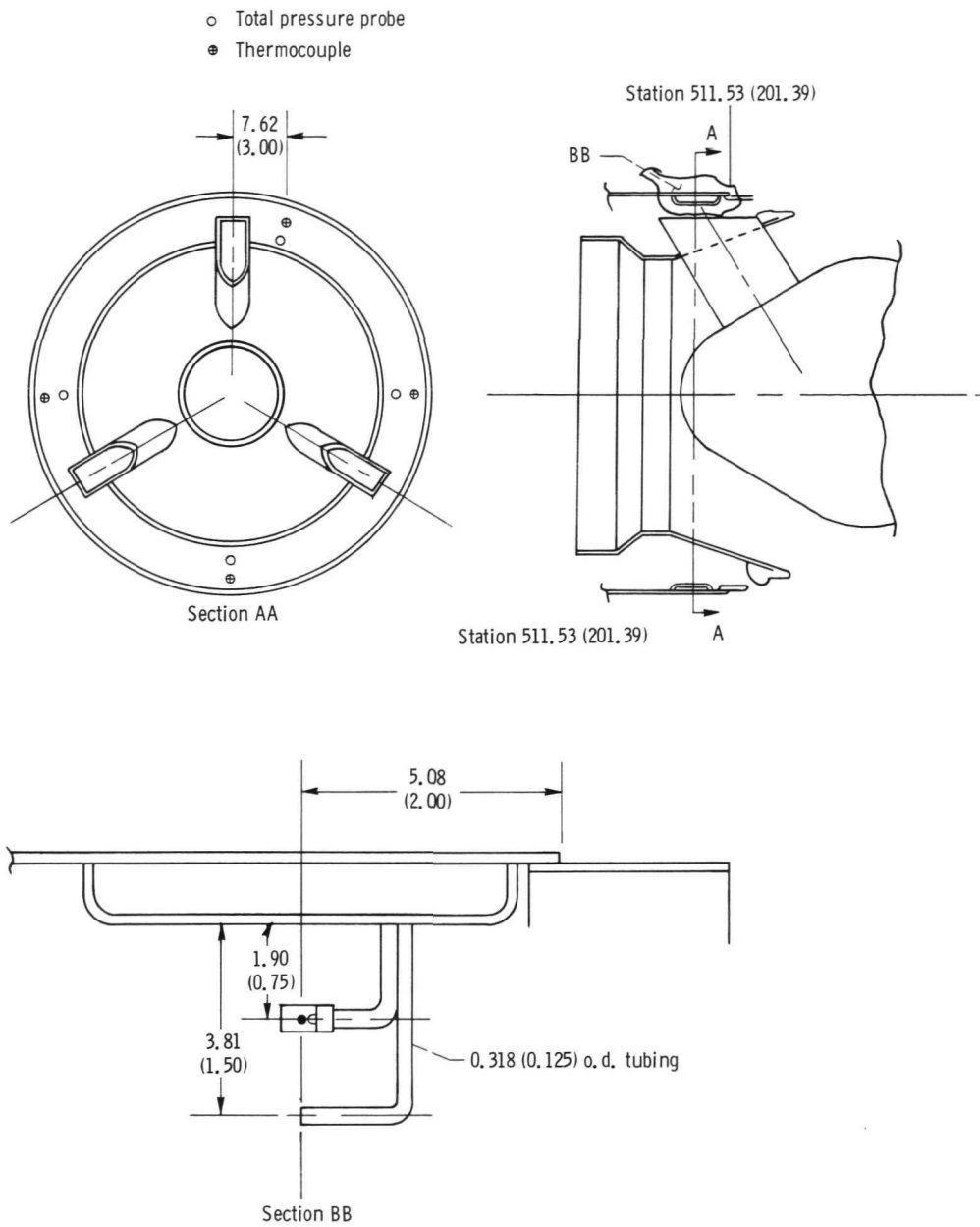
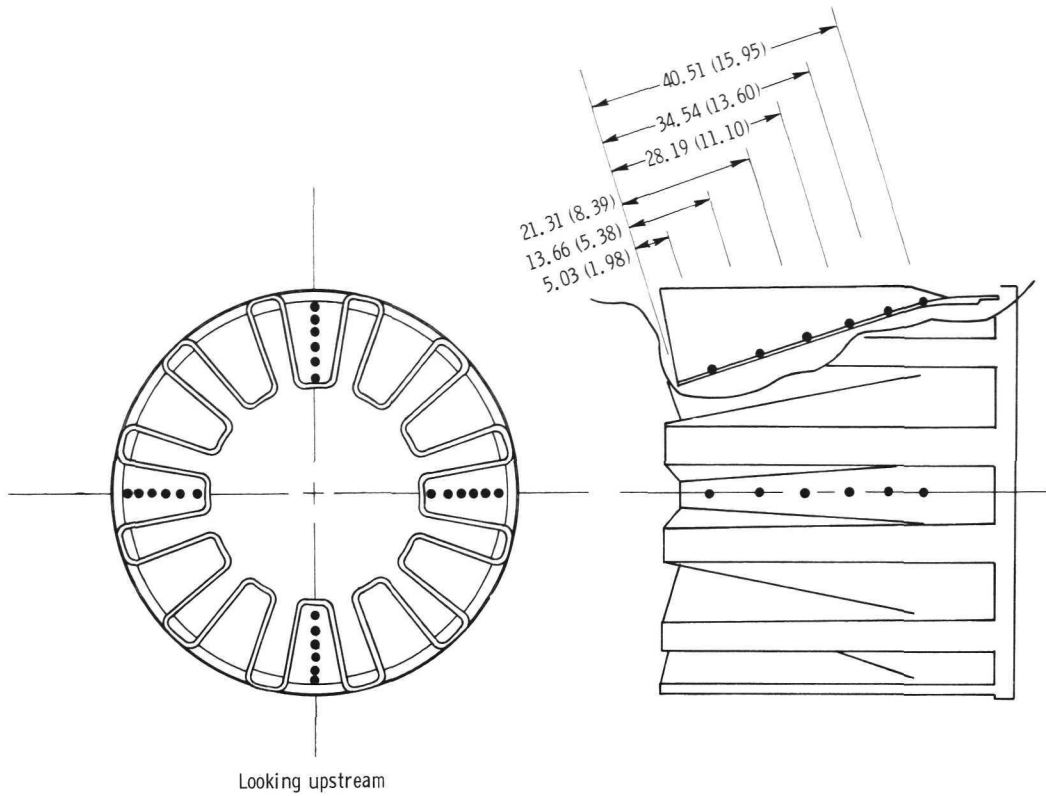
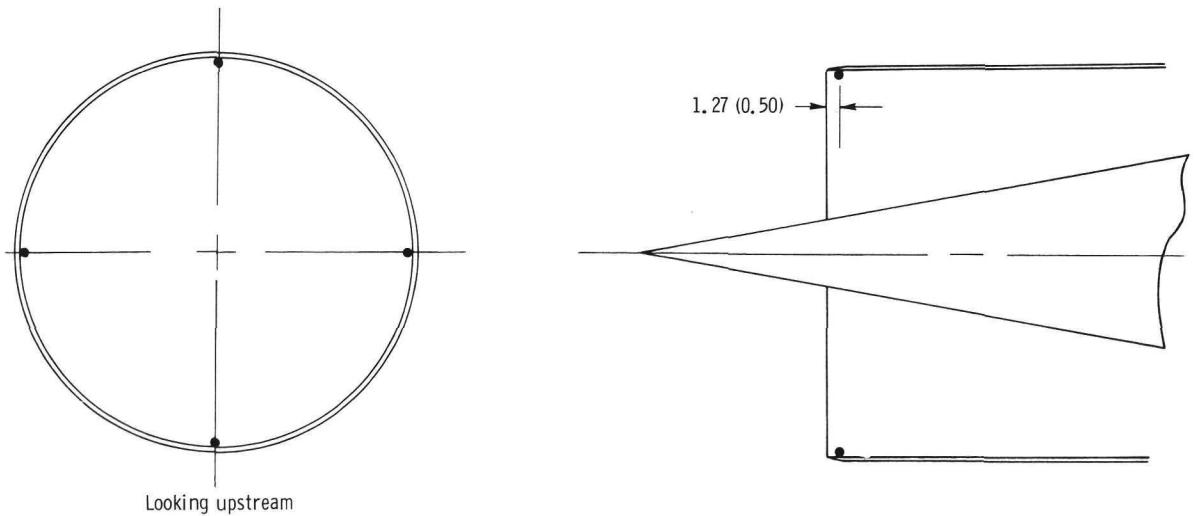


Figure 6. - Secondary passage instrumentation. (Dimensions are in cm (in.))

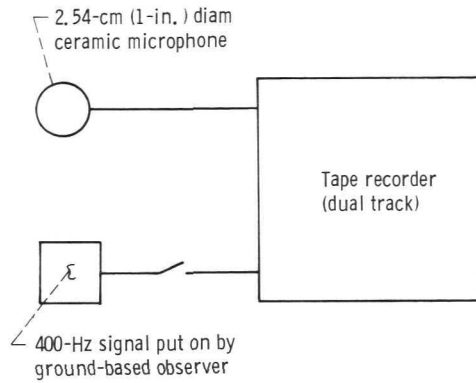


(a) Twelve-chute primary static pressure taps.

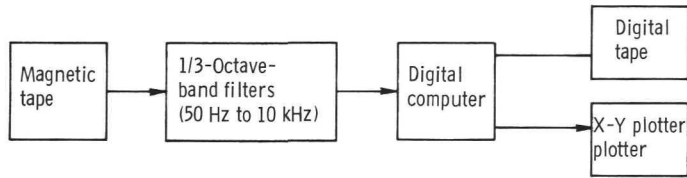


(b) Shroud static pressure taps.

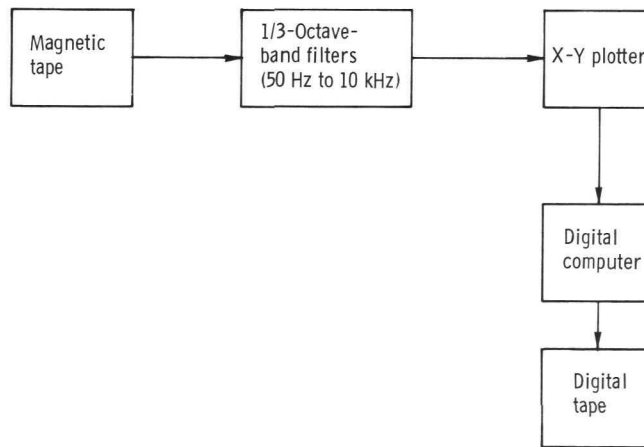
Figure 7. - Nozzle instrumentation. (Dimensions are in cm (in. ).)



(a) Recording system for both static and flyover tests.



(b) Playback system for flyover tests.

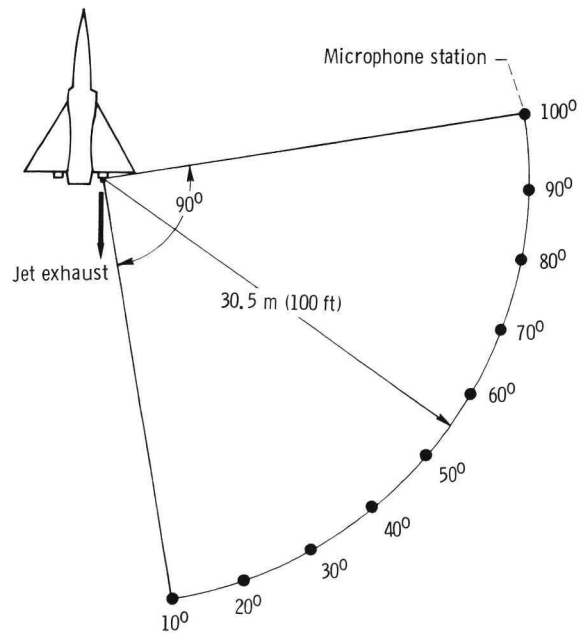


(c) Playback system for static tests.

Figure 8. - Schematic flow diagrams for noise recording system and data reduction for both static and flyover.



(a) Microphone orientation.

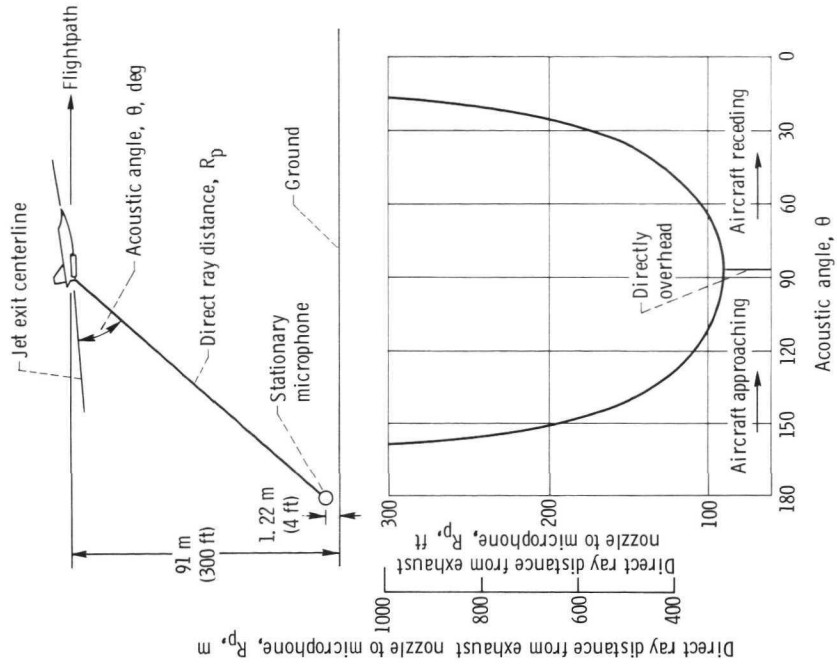


(b) Microphone location.

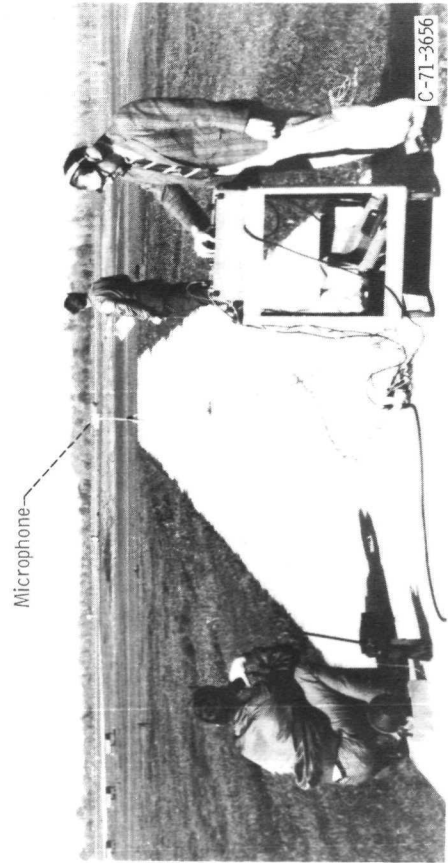
Figure 9. - Microphone orientation and location for static tests.



Figure 10. - Location of external source of cooling air for static tests.



(b) Geometry.



(a) Microphone orientation.

Figure 11. - Microphone orientation and geometry for flyover tests.

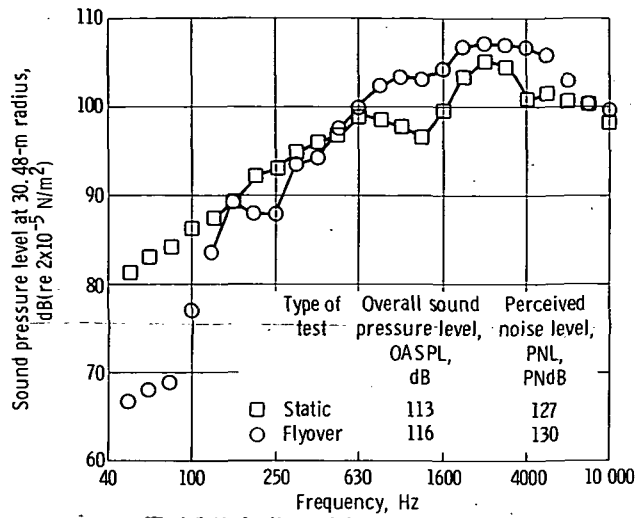


Figure 12. - Comparison of flyover and static spectra for 12-chute suppressor nozzle. Relative jet velocity,  $V_r$ , 533 m/sec (1750 ft/sec); acoustic angle (angle of peak noise for flyover);  $\theta$ ,  $50^\circ$ ; 1/3-octave bands.

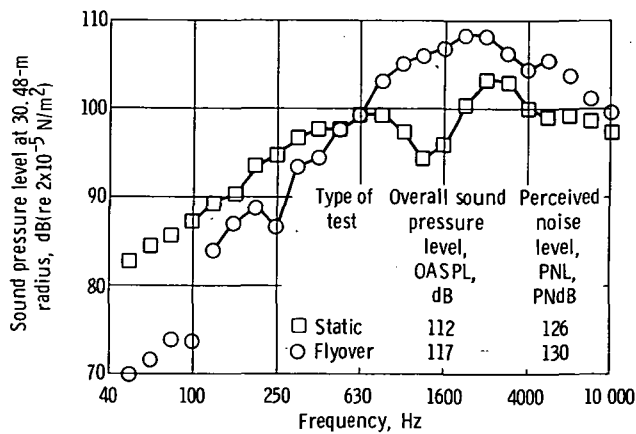
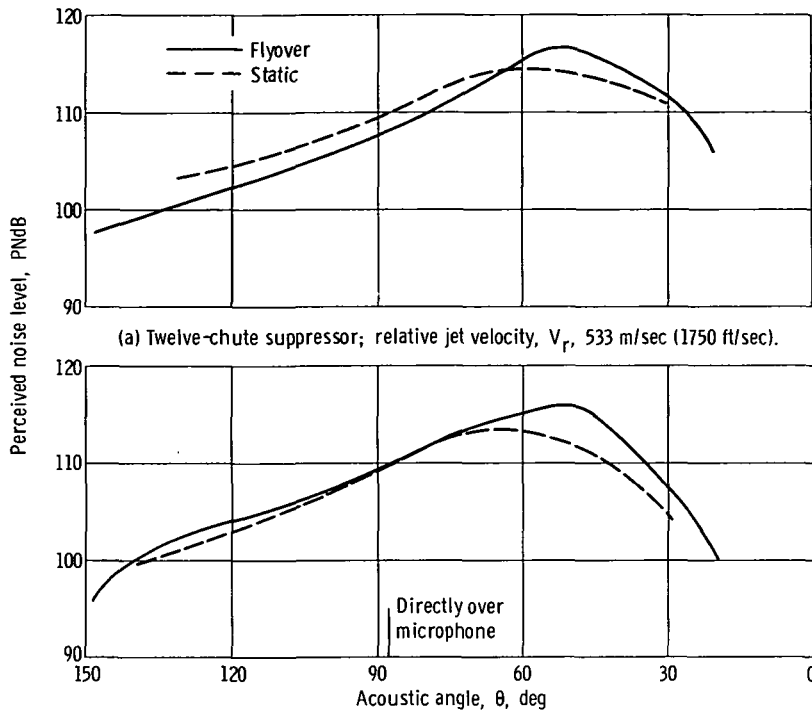


Figure 13. - Comparison of flyover and static spectra for 12-chute suppressor nozzle with hard-wall shroud. Relative jet velocity,  $V_r$ , 542 m/sec (1780 ft/sec); acoustic angle (angle of peak noise for flyover);  $\theta$ ,  $50^\circ$ ; 1/3-octave bands.



(a) Twelve-chute suppressor; relative jet velocity,  $V_r$ , 533 m/sec (1750 ft/sec).

(b) Twelve-chute suppressor with hard-wall shroud; relative jet velocity,  $V_r$ , 542 m/sec (1780 ft/sec).

Figure 14. - Flyover and static noise directivity. Comparison of typical flyover at 91-meter altitude to static data extrapolated to a 91-meter sideline. Data adjusted to free-field and standard-day conditions.

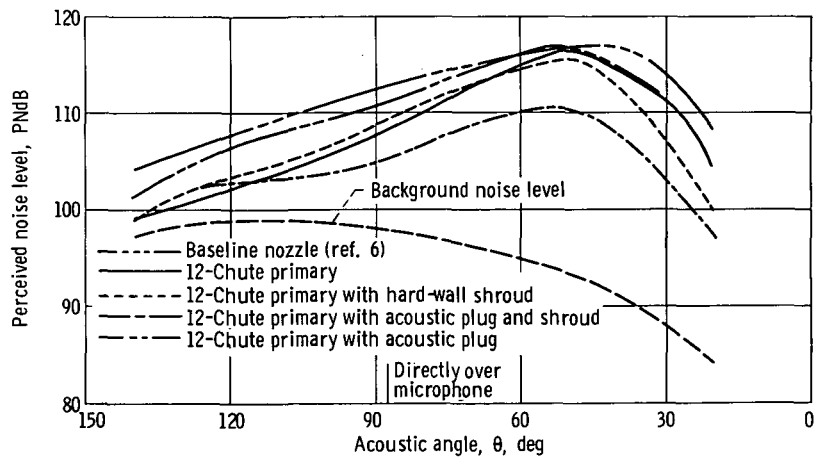


Figure 15. - Flyover noise levels directly beneath flightpath. Data adjusted to free-field, standard-day conditions. Altitude, 91 meters; relative jet velocity,  $V_r$ , 533 m/sec (1750 ft/sec).

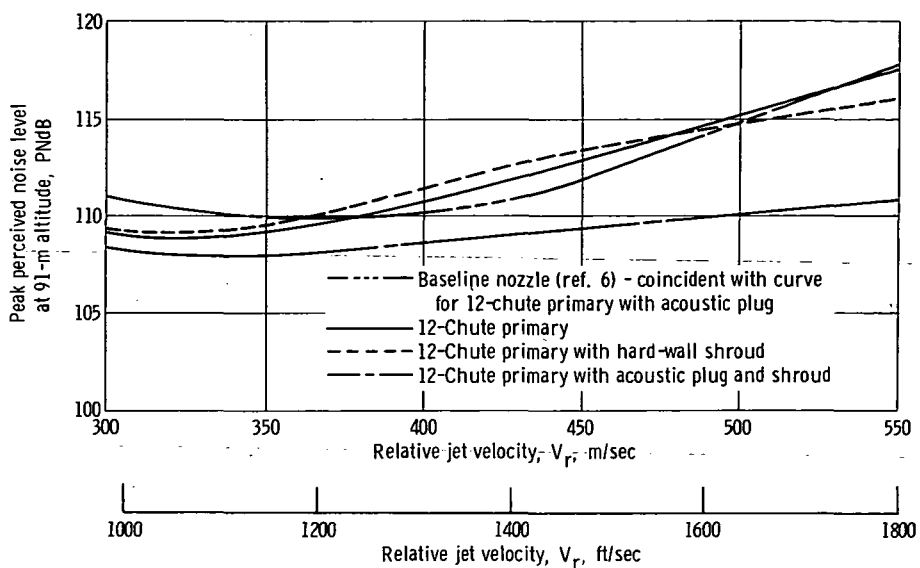


Figure 16. - Effect of relative jet velocity on peak flyover noise levels.

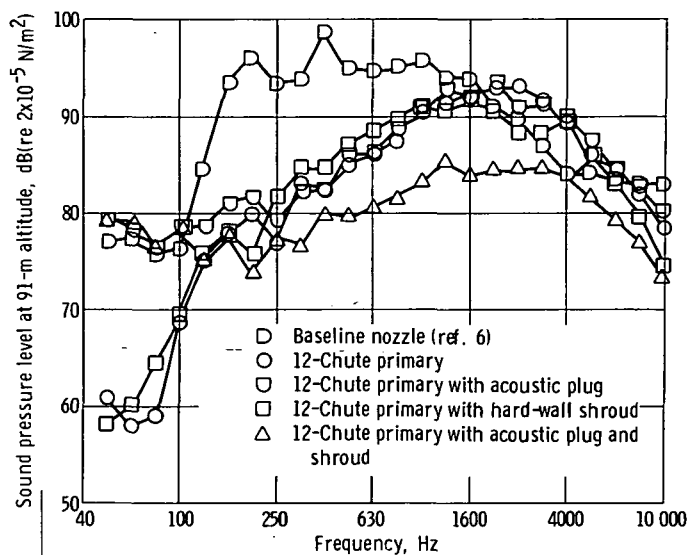
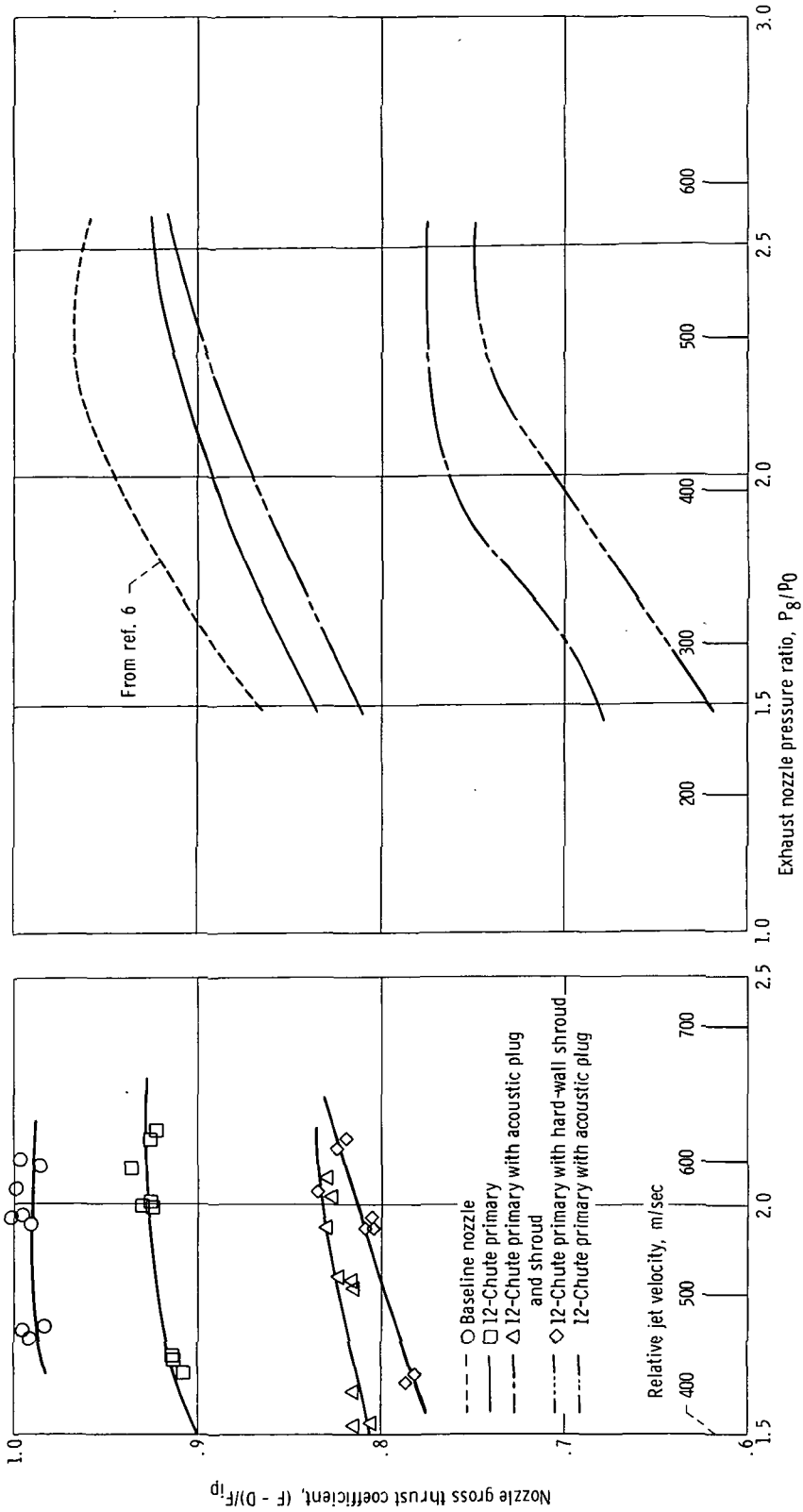
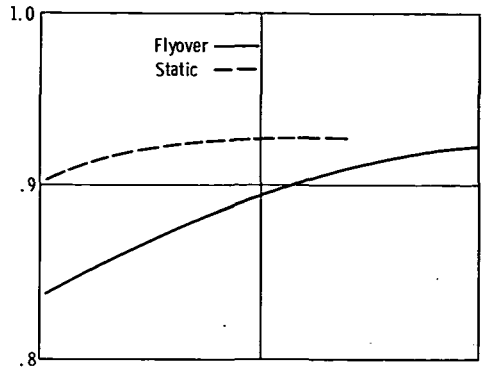


Figure 17. - Comparison of flyover spectra. Relative jet velocity,  $V_r$ , 510 m/sec (1700 ft/sec); acoustic angle (angle of peak noise for plug at flyover),  $\theta$ ,  $40^\circ$ ; 1/3-octave bands.

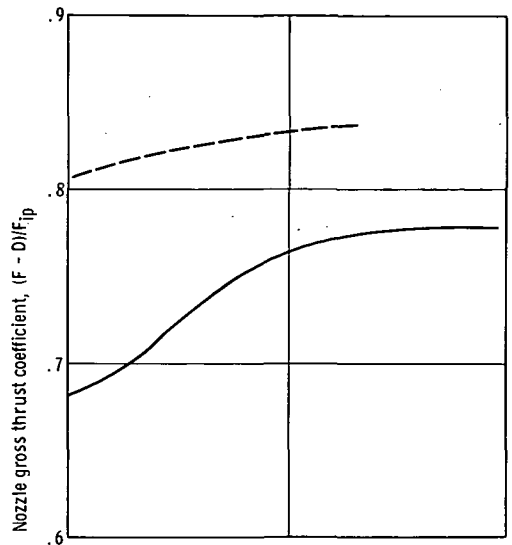


(a) Static tests. Flight Mach number,  $M_0 = 0.4$ ; corrected secondary weight flow ratio,  $\omega \sqrt{F}$ , 0.06.

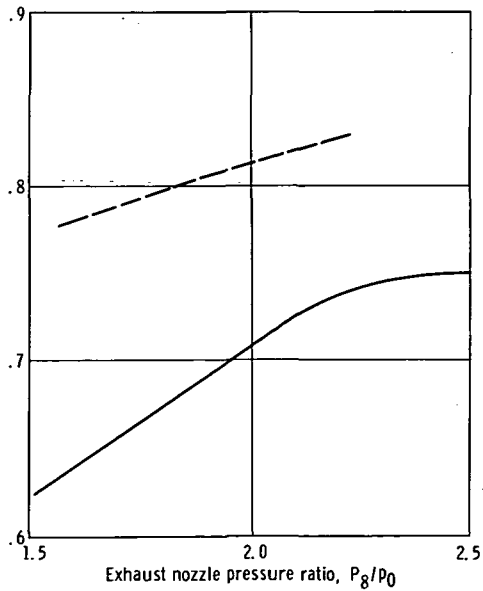
(b) Flyover tests. Thrust performance of suppressor configurations.



(a) Twelve-chute primary.



(b) Twelve-chute primary with acoustic shroud and plug.



(c) Twelve-chute primary with hard-wall shroud.

Figure 19. - Effect of flight velocity on thrust of suppressor configurations.

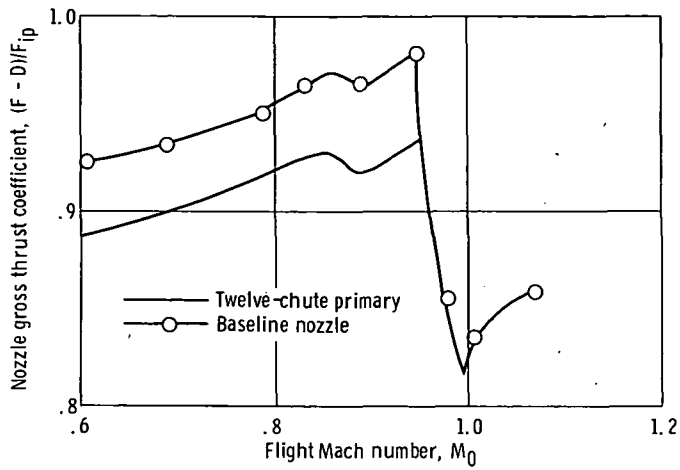


Figure 20. - Comparison of nozzle gross thrust coefficients over a range of Mach numbers. Corrected secondary weight flow ratio,  $\omega\sqrt{T}$ , 0.05; subsonic cruise.

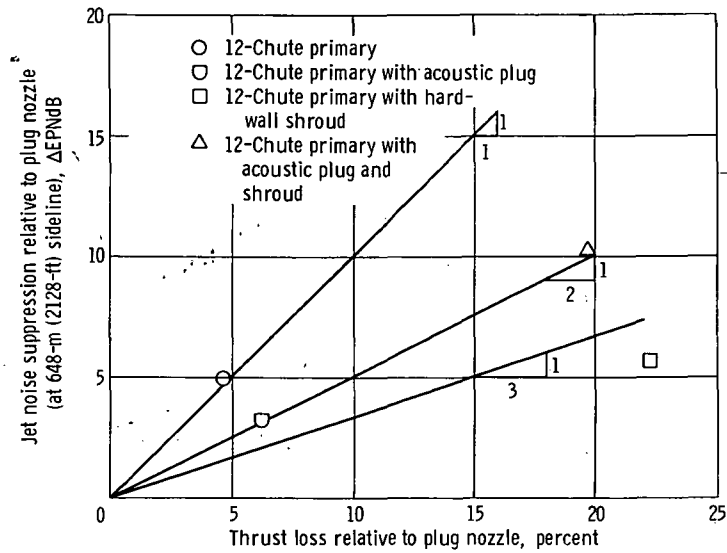


Figure 21. - Suppressor effectiveness. Flyover results scaled to four 267-kN-thrust engines; exhaust nozzle pressure ratio,  $P_8/P_0$ , 2.4; relative jet velocity,  $V_r$ , 533 m/sec (1750 ft/sec); corrected secondary weight flow ratio,  $\omega\sqrt{T}$ , 0.06; flight Mach number,  $M_0$ , 0.4.

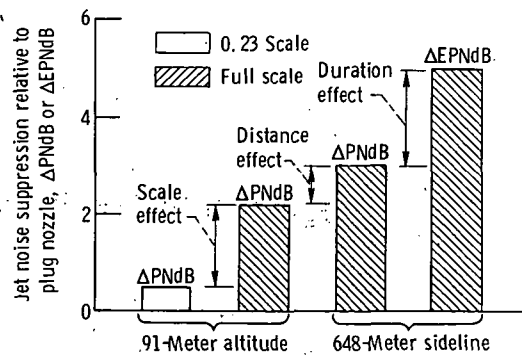


Figure 22. - Effect of scale, distance, and duration on suppression of 12-chute primary.

**Page Intentionally Left Blank**



POSTMASTER: If Undeliverable (Section 158  
Postal Manual) Do Not Return

*"The aeronautical and space activities of the United States shall be conducted so as to contribute . . . to the expansion of human knowledge of phenomena in the atmosphere and space. The Administration shall provide for the widest practicable and appropriate dissemination of information concerning its activities and the results thereof."*

—NATIONAL AERONAUTICS AND SPACE ACT OF 1958

## NASA SCIENTIFIC AND TECHNICAL PUBLICATIONS

**TECHNICAL REPORTS:** Scientific and technical information considered important, complete, and a lasting contribution to existing knowledge.

**TECHNICAL NOTES:** Information less broad in scope but nevertheless of importance as a contribution to existing knowledge.

**TECHNICAL MEMORANDUMS:** Information receiving limited distribution because of preliminary data, security classification, or other reasons. Also includes conference proceedings with either limited or unlimited distribution.

**CONTRACTOR REPORTS:** Scientific and technical information generated under a NASA contract or grant and considered an important contribution to existing knowledge.

**TECHNICAL TRANSLATIONS:** Information published in a foreign language considered to merit NASA distribution in English.

**SPECIAL PUBLICATIONS:** Information derived from or of value to NASA activities. Publications include final reports of major projects, monographs, data compilations, handbooks, sourcebooks, and special bibliographies.

**TECHNOLOGY UTILIZATION PUBLICATIONS:** Information on technology used by NASA that may be of particular interest in commercial and other non-aerospace applications. Publications include Tech Briefs, Technology Utilization Reports and Technology Surveys.

*Details on the availability of these publications may be obtained from:*

**SCIENTIFIC AND TECHNICAL INFORMATION OFFICE**

**NATIONAL AERONAUTICS AND SPACE ADMINISTRATION**

Washington, D.C. 20546